

Efficiency droop in nitride-based light-emitting diodes

Feature Article

Joachim Piprek*

NUSOD Institute LLC, Newark, Delaware 19714-7204, USA

Received 22 March 2010, revised 7 June 2010, accepted 17 June 2010
Published online 15 July 2010

Keywords Auger recombination, efficiency droop, GaN, light-emitting diodes, quantum efficiency

* Corresponding author: e-mail piprek@nusod.org, Phone: +302 565 4945, Fax: +801-207-6106

Nitride-based light-emitting diodes (LEDs) suffer from a reduction (droop) of the internal quantum efficiency with increasing injection current. This droop phenomenon is currently the subject of intense research worldwide, as it delays general lighting applications of GaN-based LEDs. Several explanations of the efficiency droop have been proposed in recent years, but none is widely accepted. This feature article provides a snapshot of the present state of droop research, reviews currently discussed droop mechanisms, contextualizes them, and proposes a simple yet unified model for the LED efficiency droop.

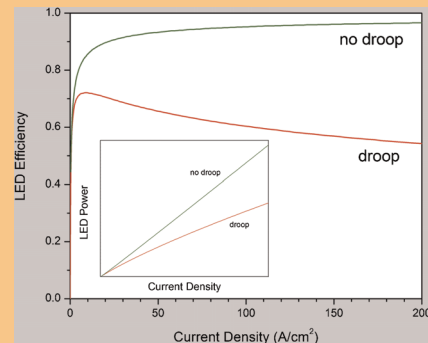


Illustration of LED efficiency droop (details in Fig. 13).

© 2010 WILEY-VCH Verlag GmbH & Co. KGaA, Weinheim

1 Introduction Since the first demonstration of InGaN/GaN light-emitting diodes (LEDs) in 1993 [1], there has been steady improvement in material quality and device fabrication so that GaN-based LEDs are now starting to enter general lighting applications [2]. A principal advantage of LED lighting over traditional lighting technologies is its high energy efficiency. However, GaN-based LEDs deliver high efficiency thus far only at low current and low brightness. At the elevated injection current required in practical high-brightness applications, the LED efficiency is substantially reduced (see figure in abstract). This efficiency droop phenomenon is observed across a broad wavelength spectrum of InGaN/GaN LEDs [3, 4] and also with deep ultraviolet (UV) AlGaN/AlN LEDs [5, 6]. Efficiency droop occurs with and without LED self-heating and it only weakly depends on the ambient temperature ($T = 4\text{--}453\text{ K}$) [7]. Many proposals have been forwarded to explain the efficiency droop. Among them are carrier delocalization [3, 4], enhanced Auger recombination [8], and electron leakage [9]. However, different sample preparation and measurement conditions as well as the application of

different models lead to a confusing and sometimes contradicting variety of efficiency droop observations and explanations. This article offers a united framework for the different droop models which helps to bring more clarity to the ongoing droop discussion.

The next section outlines a relatively simple unified model for the LED efficiency. Section 3 then reviews the main proposals to explain the droop phenomenon. Finally, Section 4 compares and discusses these droop models.

2 LED efficiency The ideal case of 100% efficiency would be accomplished when every injected electron generates a photon that is emitted from the LED. However, the transfer of electrical to optical energy is always accompanied by losses, both of electrons and of photons. Accordingly, the total (external) quantum efficiency η_{EQE} is usually split up into the internal quantum efficiency η_{IQE} and the optical extraction efficiency η_{EXE}

$$\eta_{\text{EQE}} = \eta_{\text{IQE}} \times \eta_{\text{EXE}} \quad (1)$$

The optical extraction efficiency (EXE) is the ratio of photons extracted (emitted) from the LED to photons generated inside the LED quantum wells (QWs). In other words, η_{EXE} accounts for photons lost inside the LED. It is generally believed that photon extraction is not the main cause of efficiency droop, i.e., that the internal loss of photons does not increase significantly with higher injection current. However, recent LED simulations indicate some EXE droop in thin-film LEDs [10].

The internal quantum efficiency (IQE) is the ratio of photons generated inside the QWs to the total number of electrons injected into the LED. It plays the key role in the overall efficiency droop and it therefore requires further evaluation. The IQE can be defined as the fraction of the total current I that feeds the radiative recombination inside the QW

$$\eta_{\text{IQE}} = \frac{I_{\text{rad}}}{I} = \frac{I_{\text{rad}}}{(I_{\text{rad}} + I_{\text{lost}})}. \quad (2)$$

The total current can be split up into carriers that generate photons in the QW (I_{rad}) and carriers that are lost to other processes (I_{lost}). Efficiency droop only occurs if I_{lost} increases stronger than I_{rad} with rising current injection. Thus, most droop investigations focus on possible carrier loss mechanisms in nitride LEDs.

In general, carrier losses can occur inside or outside the QWs. Non-radiative recombination processes inside the QW can either be defect-related Shockley–Read–Hall (SRH) recombination (I_{SRH}) or Auger recombination (I_{Auger}) [11]. Carrier recombination mechanisms outside the QWs are summarized as carrier leakage (I_{leak}). Thus, the total LED injection current can be split up into four parts

$$I = I_{\text{rad}} + I_{\text{SRH}} + I_{\text{Auger}} + I_{\text{leak}}, \quad (3)$$



Joachim Piprek is founder and president of the NUSOD Institute (www.nusod.org). He also serves as an executive editor of *Optical and Quantum Electronics* and co-chairs the SPIE conference on *Gallium Nitride Materials and Devices* as well as the annual conference on *Numerical Simulation of Optoelectronic Devices* (IEEE). Dr. Piprek has taught graduate courses at universities in Germany, Sweden, and in the United States. He has published three books, most recently *Nitride Semiconductor Devices: Principles and Simulation* (Wiley-VCH, 2007).

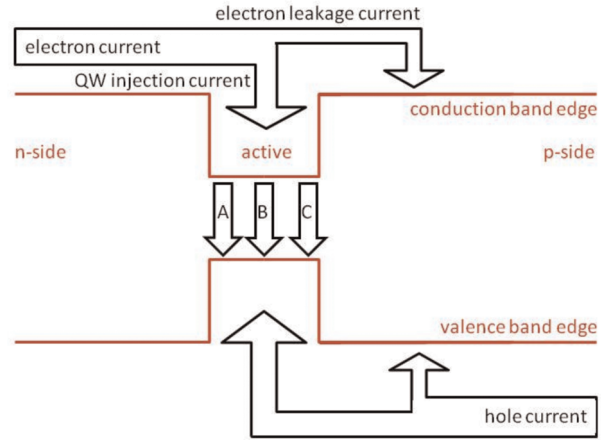


Figure 1 (online color at: www.pss-a.com) Schematic illustration of LED current components (A – SRH recombination, B – spontaneous recombination, C – Auger recombination).

which is the basis for the four principal droop mechanisms considered in the next section (Fig. 1).

The first three contributions in (3) are typically related to the simple ABC model for carrier recombination inside the QW

$$\begin{aligned} I_{\text{QW}} &= I_{\text{rad}} + I_{\text{SRH}} + I_{\text{Auger}} \\ &= qV_{\text{QW}} (An + Bn^2 + Cn^3), \end{aligned} \quad (4)$$

with the electron charge q , the active volume V_{QW} of all QWs, the QW carrier density n , the SRH parameter A , the radiative coefficient B , and the Auger coefficient C . The leakage current is hard to describe by a simple equation. Özgür et al. [12] proposed the phenomenological formula kJ^b for the leakage current density (J – total current density, k, b – fit parameters). We here use a similar formula relating the leakage current I_{leak} to the current I_{QW} injected into the QWs

$$I_{\text{leak}} = aI_{\text{QW}}^m. \quad (5)$$

This empirical approach covers carrier leakage by thermionic emission from the QWs [13], but it may also be used to describe fly-over carriers that are not captured by the QWs, or defect-assisted carrier leakage [14].

Introducing (3)–(5) into Eq. (2) leads to the unified IQE droop formula

$$\eta_{\text{IQE}} = \frac{qV_{\text{QW}} Bn^2}{(I_{\text{QW}} + aI_{\text{QW}}^m)}, \quad (6)$$

with I_{QW} given by (4). Equation (6) is equivalent to the formula

$$\eta_{\text{IQE}} = \frac{\eta_{\text{inj}} Bn^2}{(An + Bn^2 + Cn^3)}, \quad (7)$$

where the injection efficiency η_{inj} represents the fraction of carriers that recombine inside the QWs

$$\eta_{inj} = \frac{I_{QW}}{I} = \frac{I_{QW}}{(I_{QW} + aI_{QW}^m)}, \quad (8)$$

thereby accounting for carrier leakage. The total injection current density is given by

$$j = \frac{I}{A_{QW}} = \frac{(I_{QW} + aI_{QW}^m)}{A_{QW}} \quad (9)$$

with the active QW area A_{QW} . Equations (4), (6), and (9) are used in the following to generate IQE versus current density characteristics $\eta_{IQE}(j)$ for the different droop models.

3 Proposed droop mechanisms

3.1 Defect-assisted mechanisms Typical non-radiative electron–hole recombination at crystal defects is described by the SRH model [11]. The SRH carrier lifetime is equal to $1/2A$. If other carrier loss mechanisms are neglected ($I_{leak} = 0$, $C = 0$), Eq. (6) transforms into

$$\eta_{IQE} = \frac{Bn^2}{(An + Bn^2)}, \quad (10)$$

with example characteristics plotted in Fig. 2 as function of current density. The plots show that SRH recombination has a strong influence on the maximum efficiency but it does not seem to cause efficiency droop. This finding is confirmed by efficiency measurements on LEDs with different threading dislocation densities [15] as well as by dc-aging studies [16].

However, defect-related mechanisms may still contribute to efficiency droop if the A parameter itself depends on the QW carrier density, i.e., if the SRH carrier lifetime decreases with increasing carrier density. It is clear from Eq. (10) that A would need to exhibit a superlinear rise with carrier density to cause efficiency droop. Suggesting such a mechanism, early explanations of the droop phenomenon considered defect-related non-radiative recombination the main cause [3]. The idea was based on the observation of a

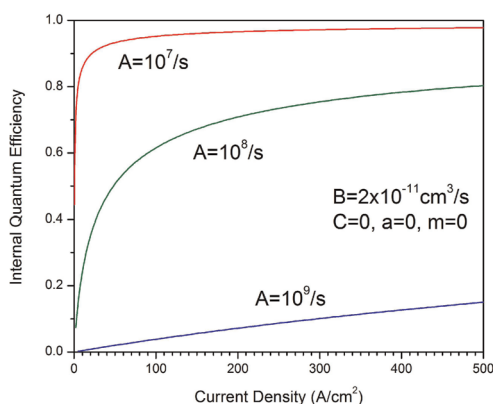


Figure 2 (online color at: www.pss-a.com) Internal quantum efficiency (10) for different parameters A .

non-uniform indium distribution inside InGaN QWs. Indium-rich clusters are associated with a lower bandgap and therefore lead to carrier localization. At low current and low QW carrier density, indium-clusters then keep carriers away from structural defects that serve as SRH recombination centers. With higher current, more carriers accumulate inside the QWs so that the indium-clusters fill up. Carriers spill over into QW regions with lower indium concentration and increasingly recombine non-radiatively at defects, leading to a SRH lifetime reduction. The existence of indium-clusters was later disputed [17], however, intentional localization of carriers inside the QW was demonstrated to reduce the droop [18]. Other authors consider V-shaped hexagonal pits which exhibit an increased bandgap that prevents QW carriers from recombining non-radiatively at low current (Fig. 3) [19]. With higher current, QW filling leads to increased recombination at these defects.

As the surprisingly low non-radiative recombination rate in InGaN QWs is still not fully understood [20], thus far undiscovered defect-related mechanisms may still be found to contribute to the droop phenomenon.

Phonon-assisted transport of holes via tunneling along dislocations was also suggested to be involved in the droop mechanism, leading to a non-radiative parasitic process that is enhanced by a local temperature rise at high injection [21]. Such a process may be included in the leakage model discussed in Section 3.4.

3.2 Spontaneous emission reduction Some researchers found that the radiative recombination mechanism contributes to the efficiency droop [22, 23]. As previously discussed in the literature [24], the spontaneous emission rate is proportional to n^2 only at low current. At higher current, it approaches a more linear dependency on n . David and Grundmann [23] employed the relationship $B = B_0/[1 + (n/n_0)]$ and extracted the parameters $B_0 = 7 \times 10^{-11} \text{ cm}^3 \text{ s}^{-1}$ and $n_0 = 5 \times 10^{18} \text{ cm}^{-3}$ from measurements on 430 nm InGaN/GaN LEDs. The resulting IQE characteristic (10) is plotted in Fig. 4 and it is compared

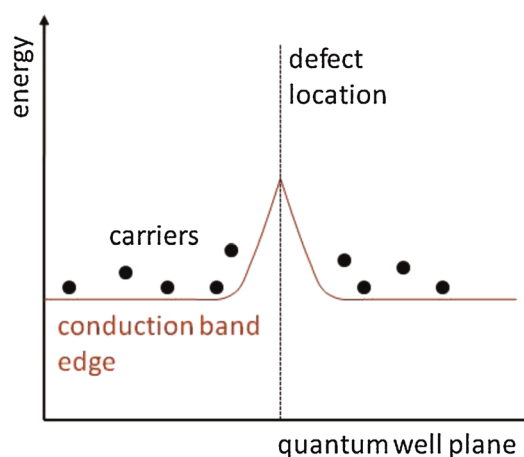


Figure 3 (online color at: www.pss-a.com) Illustration of defect self-screening from QW carriers.

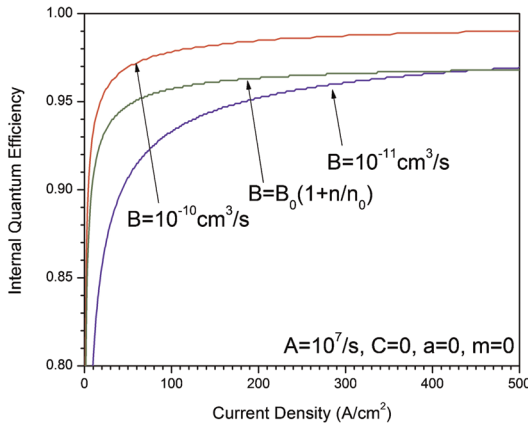


Figure 4 (online color at: www.pss-a.com) Influence of the B parameter on the IQE (10). $B_0 = 7 \times 10^{-11} \text{ cm}^3 \text{ s}^{-1}$, $n_0 = 5 \times 10^{18} \text{ cm}^{-3}$.

to the cases with constant B parameters. Obviously, the relationship $B(n)$ does not cause efficiency droop, but it lowers the barrier for non-radiative processes to trigger an efficiency reduction.

3.3 Auger recombination Non-radiative electron–hole recombination processes transfer the excess electron energy to other particles. In case of Auger recombination, these other particles are electrons or holes that are excited into higher energy levels within the same band (Fig. 5). The probability of this Auger process decreases strongly with increasing energy band gap and it is generally considered negligible in wide-gap materials. The solid dots in Fig. 6 represent Auger parameters reported for III–V compound semiconductors with band gaps smaller than in nitrides [11]. Data for the same material are scattered over several orders of magnitude (limits marked by dashed lines) which was attributed to differences in methods and models used for extraction of the Auger parameter from measurements [25]. Even considering this wide range of uncertainty, the upper limit for the GaN Auger parameter is expected near $10^{-34} \text{ cm}^6 \text{ s}^{-1}$ (band gap 3.42 eV). However, recent measurements of nitride Auger parameters give much higher numbers (open dots in Fig. 6).

The influence of Auger recombination on the efficiency droop is typically analyzed using the formula

$$\eta_{\text{IQE}} = \frac{Bn^2}{(An + Bn^2 + Cn^3)}, \quad (11)$$

Table 1 Overview of measured recombination parameters for InGaN quantum wells (λ , QW emission wavelength; A , SRH recombination; B , radiative recombination; C , Auger recombination).

authors	λ (nm)	A (s^{-1})	B ($\text{cm}^3 \text{ s}^{-1}$)	C ($\text{cm}^6 \text{ s}^{-1}$)
Zhang et al. [27]	407	1.0×10^7	2.0×10^{-11}	1.5×10^{-30}
Shen et al. [8]	440	5.4×10^7	2.0×10^{-11}	2.0×10^{-30}
Meneghini et al. [28]	450	2.3×10^7	1.0×10^{-11}	1.0×10^{-30}
Laubsch et al. [29]	523	0.47×10^7	0.12×10^{-11}	0.35×10^{-30}

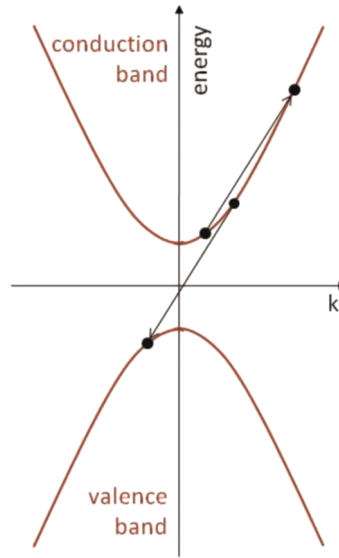


Figure 5 (online color at: www.pss-a.com) Illustration of intra-band Auger recombination (k – electron wavevector).

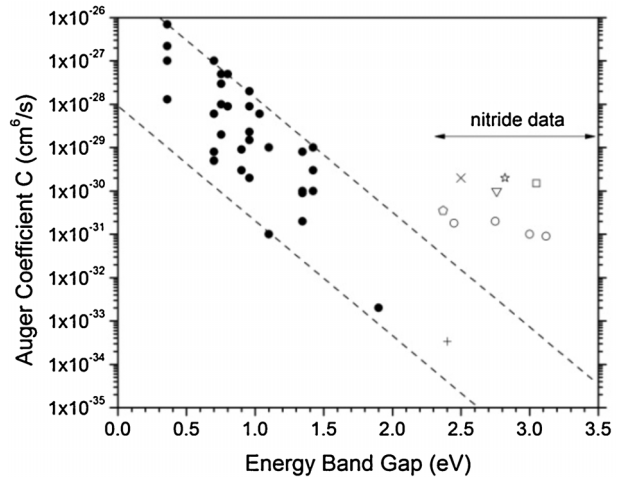


Figure 6 Auger parameters versus bandgap reported for III–V compound semiconductors. Open dots represent measurements on nitrides (star [8], circles [26], square [27], triangle [28], and pentagon [29]). The symbols + [30] and \times [32] mark calculated InGaN values. Solid dots represent other III–V materials [11].

thereby neglecting carrier leakage. The simplicity and flexibility of this ABC model contributes to its popularity. Table 1 gives an overview of recombination coefficients for InGaN QWs extracted from measurements using the ABC

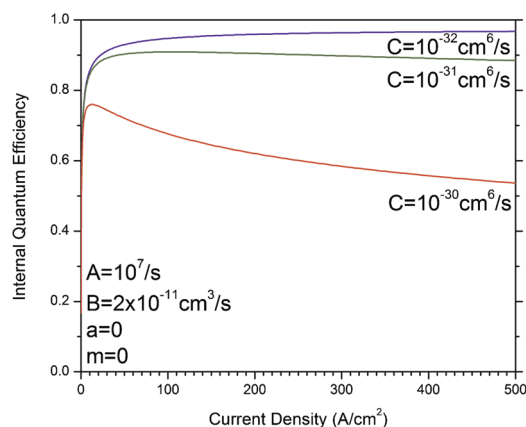


Figure 7 (online color at: www.pss-a.com) IQE plots with different Auger parameters C .

model. Figure 7 plots the result of (11) for different sets of parameters. Only Auger parameters of $10^{-31} \text{ cm}^6 \text{ s}^{-1}$ or higher cause significant efficiency droop.

First measurements of the InGaN Auger parameter were published by Shen et al. [8]. This group performed photoluminescence (PL) lifetime studies on quasi-bulk InGaN layers. An ABC rate equation model was used to extract an Auger coefficient of $C = 2 \times 10^{-30} \text{ cm}^6 \text{ s}^{-1}$ (open star in Fig. 6).

Dräger et al. [26] performed lifetime measurements on various InGaN QWs combined with an elaborate gain model to accurately determine the QW carrier density after optical excitation. They extracted Auger coefficients of about $C = 10^{-31} \text{ cm}^6 \text{ s}^{-1}$ that hardly vary with the band gap in the range 2.5–3.1 eV (open circles in Fig. 6).

Zhang et al. [27] determined the Auger coefficient of $\text{In}_{0.1}\text{Ga}_{0.9}\text{N}$ QWs from large signal modulation turn-on delay measurements on 407 nm laser diodes. They obtain a room-temperature Auger coefficient of $C = 1.5 \times 10^{-30} \text{ cm}^6 \text{ s}^{-1}$ (open square in Fig. 6).

Meneghini et al. [28] extracted QW recombination parameters from packaged 450 nm LEDs by optical power and impedance measurements leading to an Auger coefficient of $C = 10^{-30} \text{ cm}^6 \text{ s}^{-1}$ (open triangle in Fig. 6).

Laubsch et al. [29] performed electro-luminescence (EL) and resonant PL measurements on 523 nm InGaN/GaN single-QW LEDs both at very low temperature (4 K) and at room temperature (300 K). At 4 K, the peak IQE of 47% occurs at $j = 0.5 \text{ A cm}^{-2}$, followed by the typical droop. At room temperature, the peak IQE is 28% at about 2 A cm^{-2} . The authors extract exactly the same Auger coefficient of $C = 3.5 \times 10^{-31} \text{ cm}^6 \text{ s}^{-1}$ for both temperatures, concluding that the droop mechanism is not thermally activated (open pentagon in Fig. 6).

Note that all of the above measurements of the Auger parameter used the ABC model and neglected the influence of carrier leakage.

Several theoretical groups calculated the nitride Auger coefficient directly. Hader et al. [30] used a microscopic

many-body model and a relatively simple kp bandstructure model to study radiative and Auger recombination in InGaN QWs. They extract a very small coefficient of $C = 3.5 \times 10^{-34} \text{ cm}^6 \text{ s}^{-1}$ for the direct band-to-band Auger process (+ in Fig. 6). An extension of this model to phonon-assisted Auger recombination did not indicate any relevant influence of Auger recombination on the efficiency droop [31].

First-principle density-functional and many-body-perturbation theory was employed by Delaney et al. [32] who confirmed the negligible probability of conventional intra-band Auger recombination for bulk InGaN band gaps greater than 2 eV. But they also identified an interband Auger process which exhibits a peak Auger coefficient of $C = 2 \times 10^{-30} \text{ cm}^6 \text{ s}^{-1}$ in bulk InGaN with 2.5 eV band gap (\times in Fig. 6). At this energy, the distance between the two conduction bands is close to the band gap, enabling strong interband transitions (Fig. 8). But the probability of this interband Auger recombination process decreases rapidly with changing band gap and it is therefore not suitable to explain the efficiency droop phenomenon observed across a wide wavelength range.

3.4 Carrier leakage The flow of electrons beyond the QWs is a common problem in GaN-based devices and it is a reason for the typical implementation of an AlGaIn electron blocker layer (EBL) on the p-side of the multi-quantum well (MQW) active region (Fig. 9) [33]. However, the EBL is often unable to completely stop electron leakage in nitride LEDs [34]. Several publications suspected electron leakage beyond the EBL to be linked to the LED efficiency droop [35, 36].

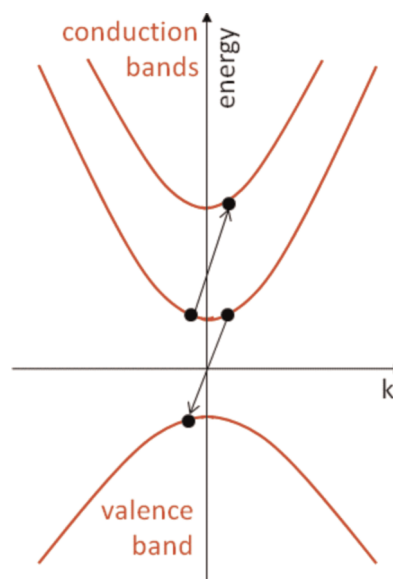


Figure 8 (online color at: www.pss-a.com) Illustration of inter-band Auger recombination (k – electron wavevector).

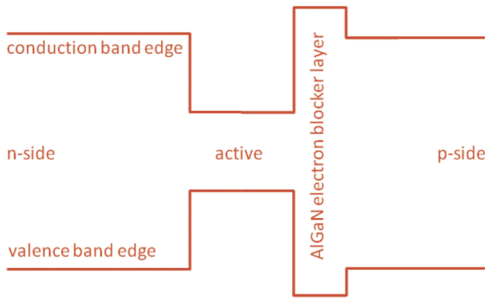


Figure 9 (online color at: www.pss-a.com) Schematic energy band diagram with electron blocking layer.

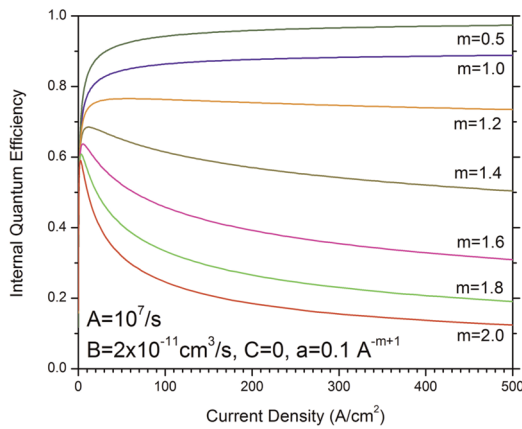


Figure 10 (online color at: www.pss-a.com) IQE (6) for different leakage parameters m .

For illustration, we here apply the formulas from Section 2 without Auger recombination ($C = 0$). Figure 10 shows the resulting IQE droop for different values of the leakage current parameter m in (6). Electron leakage causes droop only for $m > 1$ because the leakage current then rises stronger with the carrier density than the radiative recombination current.

However, earlier numerical LED device simulations did not show an efficiency droop despite the inclusion of electron leakage current [34, 37]. The main reason for the missing efficiency droop was the high band offset ratio of $\Delta E_c/\Delta E_v = 70:30$ assumed for nitride semiconductors

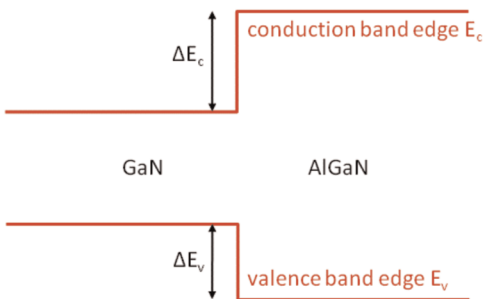


Figure 11 (online color at: www.pss-a.com) Illustration of the band offset ratio $\Delta E_c/\Delta E_v$.

(Fig. 11) [11]. In other words, the theoretically predicted EBL energy barrier was too high to allow for sufficient electron leakage. Numerical LED simulations were able to link electron leakage to efficiency droop only after reducing the AlGaN band offset ratio to 50:50 [9].

Direct experimental proof of electron leakage beyond the EBL was recently provided by measuring spontaneous emission from the p-side of the LED [38, 39]. Electrons leaking into the p-doped LED layers capture holes there before these holes reach the active region, thereby reducing hole injection into the QWs (see Fig. 1).

One of the possible reasons for electron leakage is the energy barrier reduction by built-in nitride polarization (Fig. 12) [40]. With the typical Ga-polar growth of nitride LEDs, the polarization charges at the MQW–EBL interface are positive, which leads to electron accumulation at this interface and strong negative band bending. Figure 12 shows that this polarization effect compensates for the EBL conduction band offset, even at an offset ratio of $\Delta E_c/\Delta E_v = 70:30$. The energy band diagram in Fig. 12 is calculated using non-linear polarization theory [41]. Experimental investigations of similar QWs indicate weaker polarization than predicted, ranging from 20% [42] to 80% [43] of the theoretical value, with typical results near 50% [44]. This broad variation was attributed to partial compensation of the built-in polarization by fixed defect and interface charges [45] or to inappropriate analysis of measured data [46]. It may explain the sometimes contradicting results regarding the EBL effect on LED efficiency droop. InGaN/GaN LEDs with AlGaN electron barrier layer typically exhibit higher peak efficiency [47] and higher droop onset currents [48] than similar LEDs without EBL. However, some authors find that the efficiency at elevated current density is higher in LEDs without EBL, which is attributed to improved hole injection [49]. Increasing the

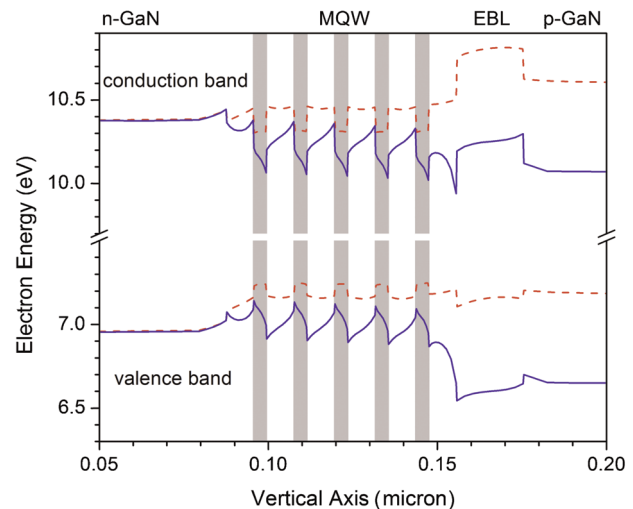


Figure 12 (online color at: www.pss-a.com) Simulated energy band diagram near the MQW active region with (solid lines) and without polarization (dashed lines). The gray areas mark the QWs.

EBL barrier height in AlGaN/AlN LEDs resulted in a significantly higher peak efficiency but it did not eliminate the droop effect [5].

Figure 12 also shows that polarization lowers the QW barriers on the p-side of each QW and thereby supports electron escape. MQW barrier p-doping was shown to reduce the efficiency droop [48, 50]. The p-side QWs seem to deliver most of the light in typical MQW LEDs [51], i.e., enhanced hole transport across the MQW gives a more uniform carrier distribution among QWs and less electron leakage.

Several proposals have been made to reduce the efficiency droop by decreasing the built-in polarization. Droop reduction was demonstrated by using polarization matched AlInGaN MQW barriers [52], partial polarization matching [53], or non-polar m-plane growth [47, 54, 55]. However, non-polar LED structures still show significant efficiency droop [56]. Low-temperature measurements on m-plane LEDs reveal acceptor freeze-out inducing hole depletion that triggers electron injection into the p-type layer at increased current, thereby leading to efficiency droop [57]. Non-polar LEDs grown on m-plane exhibit similar efficiency improvements than c-plane LEDs after EBL inclusion, suggesting that polarization is not the main factor in the efficiency degradation [47].

Some researchers consider thermally activated carrier leakage an unlikely cause of droop because the magnitude of the measured droop hardly depends on the temperature [7]. This conclusion may not be correct since rising temperatures enhance the hole transport and thereby reduce electron leakage which counteracts the usual increase in thermionic emission across the EBL with higher temperature [13].

Besides electron escape from QWs by thermionic emission, other forms of electron leakage have been discussed in connection to the efficiency droop. Some authors suspect electron tunneling through defect levels to create a leakage current path [14, 21, 58]. Others consider that electrons fly over the QW without being captured [59, 60]. Leaking electrons may have sufficient kinetic energy to even cause impact ionization in p-doped layers [61]. The approximate formula (5) may be used to describe any of these leakage mechanisms.

4 Discussion None of the above droop models is generally accepted today. The controversy is fueled in part by the contradicting results and interpretation of PL measurements. Some groups use relatively low excitation power to generate QW carrier densities close to those of electrical injection [9, 48]. They do not observe efficiency droop in these measurements and conclude that the droop mechanism is not due to processes inside the QW (such as Auger recombination). Other groups do observe efficiency droop with resonant optical excitation and attribute this to Auger recombination while neglecting leakage [7, 8]. Schubert et al. [62] argue that carrier leakage may occur even with resonant optical excitation.

Apart from discrepancies in experimental methods, both the leading droop mechanisms are also questionable from a theoretical point of view. Thus far, no convincing Auger recombination theory has been presented that justifies nitride Auger parameters close to $10^{-30} \text{ cm}^6 \text{ s}^{-1}$. All theoretical investigations of regular intraband Auger recombination result in an Auger parameter that is several orders of magnitude smaller than required for LED efficiency droop. On the other hand, numerical LED simulations show electron leakage only if the EBL conduction band offset ratio $\Delta E_c/\Delta E_v$ is lowered from 70:30 to 50:50. Band offsets between nitride alloys are hard to measure or calculate [63], however, such a reduced band offset ratio seems less unlikely than a strongly enhanced Auger recombination.

Some researchers find that Auger recombination and electron leakage are hard to distinguish in analyzing LED measurements [64]. Li and coworkers [65] demonstrated that the measured efficiency droop of various GaN-based LEDs can be reproduced employing either an electron leakage model or an Auger recombination model. We here illustrate this finding using two examples from the recent literature. Figure 13 plots $\eta_{\text{IQE}}(j)$ characteristics applying the reported parameters A , B , and C (solid lines, no leakage). Alternatively, the Auger process is replaced by leakage current (5) and the leakage parameters a and m are fitted to generate the same curves $\eta_{\text{IQE}}(j)$ (dots in Fig. 13). Obviously, Auger recombination and carrier leakage can have a very similar effect on the IQE.

Li et al. [66] have considered both Auger recombination and electron leakage in a numerical analysis of efficiency measurements. Assuming a high Auger coefficient of $C = 1.8 \times 10^{-30} \text{ cm}^6 \text{ s}^{-1}$, their simulation suggests that at

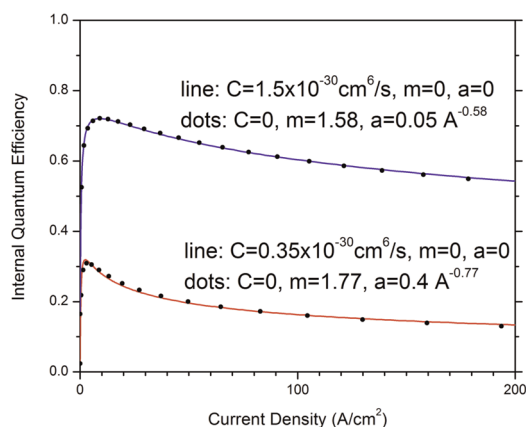


Figure 13 (online color at: www.pss-a.com) Internal quantum efficiency versus current density calculated with different parameter sets in (6). The upper line is from Zhang et al. (cf. Table 1), the dots are generated replacing Auger recombination by electron leakage. The lower line is from Laubsch et al. (cf. Table 1) and the dots are generated replacing Auger recombination by electron leakage. The upper line is also shown in the abstract figure, with and without Auger recombination.

current densities from 10 to 100 A cm⁻², Auger recombination is the dominant mechanism for efficiency droop. At current densities from 100 to 200 A cm⁻², carrier overflow becomes the dominant mechanism. The EBL band offset and polarization effects are not discussed in this paper.

As Auger recombination produces high-energy electrons far above the EBL conduction band-edge, it may lead to enhanced carrier leakage, so both mechanisms may be coupled. LED device models including such coupling have not been reported yet.

Even without a clear explanation of the underlying mechanism(s), several practical measures have been demonstrated to reduce the efficiency droop. Regardless of the employed concept, a decrease in carrier density is central to improvements of the high-current efficiency of nitride LEDs [67]. Thicker active layers were shown to push the onset of the droop effect to current densities above 200 A cm⁻² [64, 68, 69], but the efficiency is still low. Practical LED lighting applications require an IQE of about 90% at a current density of 200 A cm⁻². None of the published concepts is yet able to reach this demanding goal.

5 Conclusion Measurements are often interpreted by applying simplified mathematical models. If such models provide sufficient flexibility, their fitted agreement with experimental results is typically seen as confirmation of the physical mechanism assumed in the model. However, different models and mechanisms may be able to explain the same experimental results. It is then reasonable to consider all potential mechanisms in a unified model.

We have proposed such a unified model for the nitride LED efficiency droop. This simple model considers both Auger recombination and carrier leakage as potential explanations of the efficiency droop. As both of these explanations exhibit some weaknesses, the search for additional and improved models of the LED efficiency droop continues.

References

- [1] S. Nakamura, M. Senoh, and T. Mukai, *Jpn. J. Appl. Phys.* **23**, L8–L11 (1993).
- [2] J. Y. Tsao, in: *Solid-State Lighting: Science, Technology and Economic Perspectives*, OPTO Plenary Presentation (SPIE Photonics West, San Francisco, 2010).
- [3] T. Mukai, M. Yamada, and S. Nakamura, *Jpn. J. Appl. Phys. Part 1* **38**, 3976–3981 (1999).
- [4] Y. Yang, X. A. Cao, and C. Yan, *IEEE Trans. Electron Devices* **55**, 1771 (2008).
- [5] W. Sun, M. Shatalov, J. Deng, X. Hu, J. Yang, A. Lunev, Y. Bilenko, M. Shur, and R. Gaska, *Appl. Phys. Lett.* **96**, 061102 (2010).
- [6] H. Hirayama, S. Fujikawa, N. Noguchi, J. Norimatsu, T. Takano, K. Tsubaki, and N. Kamata, *Phys. Status Solidi A* **206**, 1176 (2009).
- [7] A. Laubsch, M. Sabathil, W. Bergbauer, M. Strassburg, H. Lugauer, M. Peter, S. Lutgen, N. Linder, K. Streubel, J. Hader, J. V. Moloney, B. Pasenow, and S. W. Koch, *Phys. Status Solidi C* **6**, S913 (2009).
- [8] Y. C. Shen, G. O. Mueller, S. Watanabe, N. F. Gardner, A. Munkholm, and M. R. Krames, *Appl. Phys. Lett.* **91**(14), 141101 (2007).
- [9] M. H. Kim, M. F. Schubert, Q. Dai, J. K. Kim, E. F. Schubert, J. Piprek, and Y. Park, *Appl. Phys. Lett.* **91**, 183507 (2007).
- [10] M. V. Bogdanov, K. A. Bulashevich, O. V. Khokhlev, I. Yu. Evstratov, M. S. Ramm, and S. Yu. Karpov, *Phys. Status Solidi C JOT* **7884** to be published (2010).
- [11] J. Piprek, *Semiconductor Optoelectronic Devices: Introduction to Physics and Simulation* (Academic Press, San Diego, 2003).
- [12] Ü. Özgür, H. Liu, X. Li, X. Ni, and H. Morkoc, in: *Proceedings of the IEEE*, **98**(7), 1180–1196 (2010).
- [13] J. Piprek and S. Li, in: *IEEE Proceedings of the 10th International Conference on Numerical Simulation of Optoelectronic Devices*, Atlanta (2010), to be published.
- [14] Y. Yang, X. A. Cao, and C. H. Yan, *Appl. Phys. Lett.* **94**, 041117 (2009).
- [15] M. F. Schubert, S. Chhajer, J. K. Kim, E. F. Schubert, D. D. Koleske, M. H. Crawford, S. R. Lee, A. J. Fischer, G. Thaler, and M. A. Banas, *Appl. Phys. Lett.* **91**, 231114 (2007).
- [16] X. Shao, H. Lu, D. Chen, Z. Xie, R. Zhang, and Y. Zheng, *Appl. Phys. Lett.* **95**, 163504 (2009).
- [17] C. J. Humphreys, *Philos. Mag.* **87**, 1971 (2007).
- [18] T. H. Hsueh, J. K. Sheu, W.-C. Lai, Y. T. Wang, H. C. Kuo, and S. C. Wang, *IEEE Photonics Technol. Lett.* **21**, 414 (2009).
- [19] A. Hangleiter, C. Netzel, D. Fuhrmann, F. Hitzel, L. Hoffmann, H. Bremers, U. Rossow, G. Ade, and P. Hinze, *Philos. Mag.* **87**, 2041 (2007).
- [20] S. F. Chichibu, A. Uedono, T. Onuma, B. A. Haskell, A. Chakraborty, T. Koyama, P. T. Fini, S. Keller, S. P. DenBaars, J. S. Speck, U. K. Mishra, S. Nakamura, S. Yamaguchi, S. Kamiyama, H. Amano, I. Akasaki, J. Han, and T. Sota, *Nature Mater.* **5**, 810 (2006).
- [21] B. Monemar and B. E. Sernelius, *Appl. Phys. Lett.* **91**, 181103 (2007).
- [22] J. I. Shim, H. Kim, and H. Y. Ryu, “Explanation of the efficiency droop in InGaN multiple quantum well light-emitting diodes by the reduced radiative recombination probability”, Presentation at SPIE Photonics West, Conf. 7617, San Francisco, January 2010.
- [23] A. David, and M. J. Grundmann, *Appl. Phys. Lett.* **96**, 103504 (2010).
- [24] J. Hader, J. V. Moloney, and S. W. Koch, *Appl. Phys. Lett.* **87**, 201112 (2005).
- [25] J. Piprek, P. Abraham, and J. E. Bowers, *IEEE J. Quantum Electron.* **36**, 366 (2000).
- [26] A. D. Dräger, H. Jönen, C. Netzel, U. Rossow, and A. Hangleiter, 8th International Conference on Nitride Semiconductors, Jeju (2009).
- [27] M. Zhang, P. Bhattacharya, J. Singh, and J. Hinckley, *Appl. Phys. Lett.* **95**, 201108 (2009).
- [28] M. Meneghini, N. Trivellin, G. Meneghesso, and E. Zanoni, *J. Appl. Phys.* **106**, 114508 (2009).
- [29] A. Laubsch, M. Sabathil, J. Baur, M. Peter, and B. Hahn, *IEEE Trans. Electron Devices* **57**, 79 (2010).
- [30] J. Hader, J. V. Moloney, B. Pasenow, S. W. Koch, M. Sabathil, N. Linder, and S. Lutgen, *Appl. Phys. Lett.* **92**(26), 261103 (2008).
- [31] S. Koch, private communication.
- [32] K. T. Delaney, P. Rinke, and C. G. Van de Walle, *Appl. Phys. Lett.* **94**, 191109 (2009).

- [33] J. Piprek and S. Nakamura, *IEE Proc. Optoelectron.* **149**, 145 (2002).
- [34] J. Piprek and S. Li, in: *Optoelectronic Devices: Advanced Simulation and Analysis*, edited by J. Piprek (Springer, New York, 2005), Chap. 10.
- [35] A. E. Yunovich, V. E. Kudryashov, A. N. Turkin, A. Kovalev, and F. Manyakhin, *MRS Int. J. Nitride Semicond. Res.* **3**, 44 (1998).
- [36] I. V. Rozhansky and D. A. Zakheim, *Phys. Status Solidi A* **204**, 227 (2007).
- [37] K. A. Bulashevich, V. F. Mymrin, S. Yu. Karpov, I. A. Zhmakin, and A. I. Zhmakin, *J. Comput. Phys.* **213**, 214 (2006).
- [38] A. Knauer, F. Brunner, T. Kolbe, V. Küller, H. Rodriguez, S. Einfeldt, M. Weyers, and M. Kneissl, *Proc. SPIE* **7231**, 72310G (2009).
- [39] K. J. Vampola, M. Iza, S. Keller, S. P. DenBaars, and S. Nakamura, *Appl. Phys. Lett.* **94**, 061116 (2009).
- [40] J. Piprek, R. Farrell, S. DenBaars, and S. Nakamura, *IEEE Photonics Technol. Lett.* **18**, 7 (2006).
- [41] V. Fiorentini, F. Bernardini, and O. Ambacher, *Appl. Phys. Lett.* **80**, 1204 (2002).
- [42] S. F. Chichibu, A. C. Abare, M. S. Minsky, S. Keller, S. B. Fleischer, J. E. Bowers, E. Hu, U. K. Mishra, L. A. Coldren, S. P. DenBaars, and T. Sota, *Appl. Phys. Lett.* **73**, 2006 (1998).
- [43] F. Renner, P. Kiesel, G. H. Döhler, M. Kneissl, C. G. Van de Walle, and N. M. Johnson, *Appl. Phys. Lett.* **81**, 490–492 (2002).
- [44] H. Zhang, E. J. Miller, E. T. Yu, C. Poblenz, and J. S. Speck, *Appl. Phys. Lett.* **84**, 4644–4646 (2004).
- [45] J. P. Ibbetson, P. T. Fini, K. D. Ness, S. P. DenBaars, J. S. Speck, and U. K. Mishra, *Appl. Phys. Lett.* **77**, 250 (2000).
- [46] I. H. Brown, I. A. Pope, P. M. Smowton, P. Blood, J. D. Thomson, W. W. Chow, D. P. Bour, and M. Kneissl, *Appl. Phys. Lett.* **86**, 131108 (2005).
- [47] J. Lee, X. Li, X. Ni, Ü. Özgür, H. Morkoç, T. Paskova, G. Mulholland, and K. R. Evans, *Appl. Phys. Lett.* **95**, 201113 (2009).
- [48] J. Xie, X. Ni, Q. Fan, R. Shimada, Ü. Özgür, and H. Morkoç, *Appl. Phys. Lett.* **93**, 121107 (2008).
- [49] S. H. Han, D. Y. Lee, S. J. Lee, C. Y. Cho, M. K. Kwon, S. P. Lee, D. Y. Noh, D. J. Kim, Y. C. Kim, and S. J. Park, *Appl. Phys. Lett.* **94**, 231123 (2009).
- [50] X. Ni, Q. Fan, R. Shimada, U. Ozgur, and H. Morkoc, *Appl. Phys. Lett.* **93**, 171113 (2008).
- [51] A. David, M. J. Grundmann, J. F. Kaeding, N. F. Gardner, T. G. Mihopoulos, and M. K. Krames, *Appl. Phys. Lett.* **92**, 053502 (2008).
- [52] M. F. Schubert, J. Xu, J. K. Kim, E. F. Schubert, M. H. Kim, S. Yoon, S. M. Lee, C. Sone, T. Sakong, and Y. Park, *Appl. Phys. Lett.* **93**, 041102 (2008).
- [53] M. H. Kim, W. Lee, D. Zhu, M. F. Schubert, J. K. Kim, E. F. Schubert, and Y. Park, *IEEE J. Sel. Top. Quantum Electron.* **15**, 1 (2009).
- [54] M. C. Schmidt, K.-C. Kim, H. Sato, N. Fellows, H. Masui, S. Nakamura, S. P. DenBaars, and J. S. Speck, *Jpn. J. Appl. Phys.* **46**, L126 (2007).
- [55] X. Li, X. Ni, J. Lee, M. Wu, Ü. Özgür, H. Morkoç, T. Paskova, G. Mulholland, and K. R. Evans, *Appl. Phys. Lett.* **95**, 121107 (2009).
- [56] H. Masui, S. Nakamura, S. P. DenBaars, and U. K. Mishra, *IEEE Trans. Electron Devices* **57**, 88 (2010).
- [57] H. Masui, H. Kroemer, M. C. Schmidt, K.-C. Kim, N. N. Fellows, S. Nakamura, and S. P. DenBaars, *J. Phys. D* **41**, 082001 (2008).
- [58] N. I. Bochkareva, V. V. Voronenkov, R. I. Gorbunov, A. S. Zubrilov, Y. S. Lelikov, P. E. Latyshev, and Y. T. Rebane, I. A. I. Tsyuk, Y. G. Shreter, *Appl. Phys. Lett.* **96**, 133502 (2010).
- [59] S. Steiger, R. G. Veprek, and B. Witzigmann, *J. Comput. Electron.* **7**, 509 (2008).
- [60] X. Ni, X. Li, J. Lee, S. Liu, V. Avrutin, Ü. Özgür, H. Morkoç, A. Matulionis, T. Paskova, G. Mulholland, and K. R. Evans, *Phys. Status Solidi RRL* **4**(8/9), 194 (2010) (DOI: 10.1002/pssr.201004147).
- [61] H. Masui, H. Sato, H. Asamizu, M. C. Schmidt, N. N. Fellows, S. Nakamura, and S. P. DenBaars, *Jpn. J. Appl. Phys.* **46**, L627 (2007).
- [62] M. F. Schubert, J. Xu, Q. Dai, F. W. Mont, J. K. Kim, and E. F. Schubert, *Appl. Phys. Lett.* **94**, 081114 (2009).
- [63] J. Piprek (ed.) *Nitride Semiconductor Devices: Principles and Simulation* (Wiley-VCH, Berlin, 2007), Chap. 2.
- [64] M. Maier, K. Köhler, M. Kunzer, W. Pletschen, and J. Wagner, *Appl. Phys. Lett.* **94**, 041103 (2009).
- [65] X. Li, H. Liu, X. Ni, Ü. Özgür, and H. Morkoç, *Superlattices Microstruct.* **47**, 118 (2010).
- [66] Y.-L. Li, Y.-R. Huang, and Y.-H. Lai, *IEEE J. Sel. Top. Quantum Electron.* **15**, 1128 (2009).
- [67] A. Laubsch, W. Bergbauer, M. Sabathil, M. Strassburg, H. Lugauer, M. Peter, T. Meyer, Ge. Brüderl, J. Wagner, N. Linder, K. Streubel, and B. Hahn, *Phys. Status Solidi C* **6**, S885 (2009).
- [68] N. F. Gardner, G. O. Müller, Y. C. Shen, G. Chen, S. Watanabe, W. Götz, and M. R. Krames, *Appl. Phys. Lett.* **91**, 243506 (2007).
- [69] K. A. Bulashevich and S. Yu. Karpov, *Phys. Status Solidi C* **5**, 2066 (2008).